Stanford Exploration Project, Report 79, November 16, 1997, pages 153–161

Four-pass technique for 3-D omega-x-y migration

Li Teng and Gopal Palacharla[1]

keywords: *three-dimensional, dispersion, approximation*

ABSTRACT

This paper tests Ristow's four-pass method of 3-D migration as an improvement on the conventional two-pass finite-difference migration. The four-pass technique consists of applying the forty-five degree finite-difference operator along the inline and crossline directions and along the other two directions at forty-five degree azimuth to the inline and crossline directions. We have derived the dispersion relation and differential equations for the four-pass technique and implemented the four-pass technique. The results show that the four-pass operator is more isotropic than the two-pass one.

INTRODUCTION

Depth extrapolation of the one-way wave equation in three dimensions can be carried out using finite-difference methods in the (ω, x, y) domain. The implicit formulation of the 3-D problem produces a block tridiagonal system of equations (Claerbout, 1985). Since the direct solution of this system is an expensive process, the usual technique used in carrying out the extrapolation is the splitting technique. Splitting in three dimensions is based on an approximation that enables the full 3-D operator to be realized by applying the 2-D operator along x for all y and then along y for all x. This technique yields an operator that is anisotropic, with the greatest error at the 45 degree azimuth.

In Yilmaz's book (1988), we found the reference to Ristow's four-pass technique (Ristow, 1980), in which the forty-five degree finite-difference operator was applied not only along the two conventional axes but also along the axes rotated to 45 degree azimuth from the original axes to compensate the greatest error at 45 degree azimuth. This paper tests this method and compares the results of the two-pass method and the four-pass method. In the future, we plan to compare it to the Hale-McClellan method.

[1]**email:** not available

DERIVATION OF THE FOUR-PASS EQUATION

Starting with the 3-D dispersion relation, we derive the equation for the four-pass technique in the wavenumber domain. We then make a contour plot to study the isotropy of the operator. The exact dispersion relation in three dimensions in terms of the dimensionless quantity vk/ω is expressed by the following equation:

$$\frac{vk_z}{\omega} = \sqrt{1 - \frac{v^2k_x^2}{\omega^2} - \frac{v^2k_y^2}{\omega^2}} \tag{1}$$

The splitting approximation of the 3-D dispersion relation (Brown, 1983) is given by

$$\frac{vk_z}{\omega} = \left[\sqrt{1 - \frac{v^2k_x^2}{\omega^2}} + \sqrt{1 - \frac{v^2k_y^2}{\omega^2}} - 1\right] \tag{2}$$

The 45-degree approximation of the 3-D dispersion relation with splitting is

$$\frac{vk_z}{\omega} = 1 - \frac{\frac{v^2}{\omega^2}k_x^2}{2 - \frac{v^2k_x^2}{2\omega^2}} - \frac{\frac{v^2}{\omega^2}k_y^2}{2 - \frac{v^2k_y^2}{2\omega^2}} \tag{3}$$

In Figure 1, the solid line shows the contours of vk_z/ω for the exact dispersion relation of equation (1); the dashed line, the splitting approximation for the 3-D dispersion relation of equation (2); and the dotted line, the 45-degree splitting approximation for the 3-D dispersion relation of equation (3). The splitting approximations show the familiar anisotropy in relation to the azimuth. The greatest error appears at 45 degree azimuth.

After an azimuth rotation of 45 degrees, as shown in Figure **??**, the 45-degree approximation for the split 3-D dispersion relation can be obtained as follows:

$$k_x' = k_x \cos\theta + k_y \sin\theta \tag{4}$$

$$k_y' = -k_x \cos\theta + k_y \sin\theta \tag{5}$$

where k_x' and k_y' are the new axes after a rotation by angle θ. For $\theta = 45$ degrees, substituting the following relations

$$k_x' = \frac{k_x}{\sqrt{2}} + \frac{k_y}{\sqrt{2}} \tag{6}$$

$$k_y' = -\frac{k_x}{\sqrt{2}} + \frac{k_y}{\sqrt{2}} \tag{7}$$

into Equation (3) gives

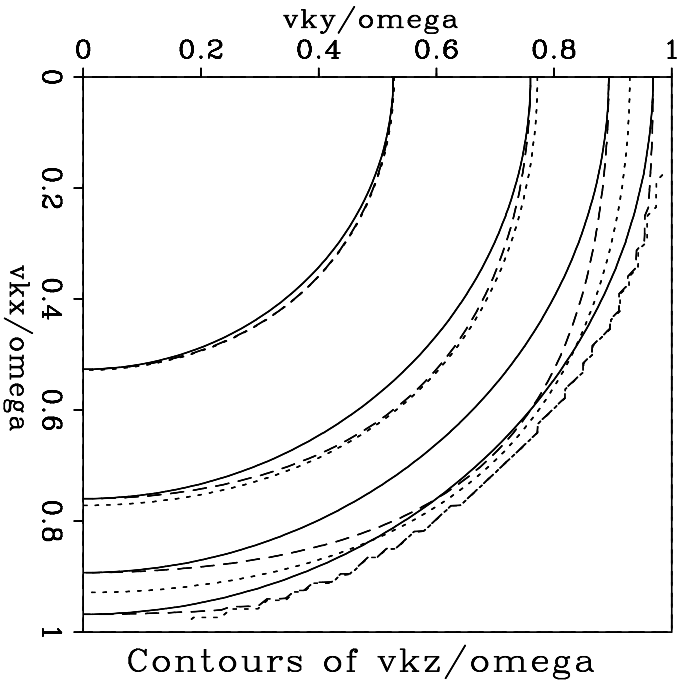

Figure 1: Contours of constant amplitude and phase for the exact 3-D dispersion relation described in equation (1) (solid line), the splitting approximation in equation (2) (dashed line), and the 45-degree approximation to splitting in equation (3) (dotted line). tengli-exac-split-45 [ER]

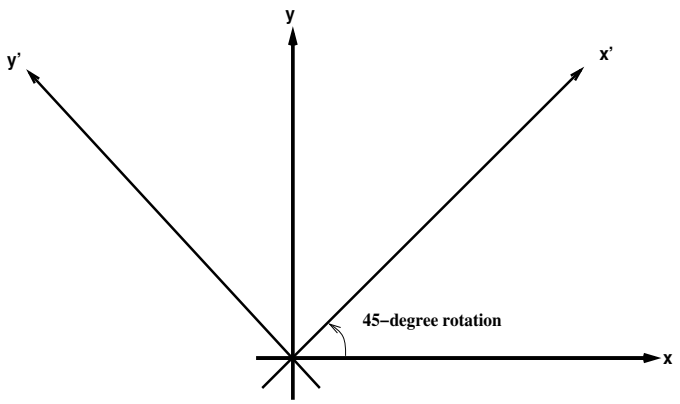

Figure 2: The rotation from (x, y) coordinate system to (x', y') system. tengli-coord [NR]

$$\frac{vk_z}{\omega} = 1 - \frac{\frac{1}{2}\frac{v^2}{\omega^2}(k_x + k_y)^2}{2 - \frac{v^2(k_x+k_y)^2}{4\omega^2}} - \frac{\frac{1}{2}\frac{v^2}{\omega^2}(-k_x + k_y)^2}{2 - \frac{v^2(-k_x+k_y)^2}{4\omega^2}} \tag{8}$$

Figure 3 shows the contours of vk_z/ω for the 45-degree approximation, with an azimuth rotation of 45 degrees (the dashed line) and without (the solid line). The curves of the two approximations have their greatest errors at different places. For the one without rotation, the worst error is at the 45 degree azimuth; for the one with 45 degree rotation, the worst error is along x and y axes. Therefore, the average of the two should give us a more isotropic operator.

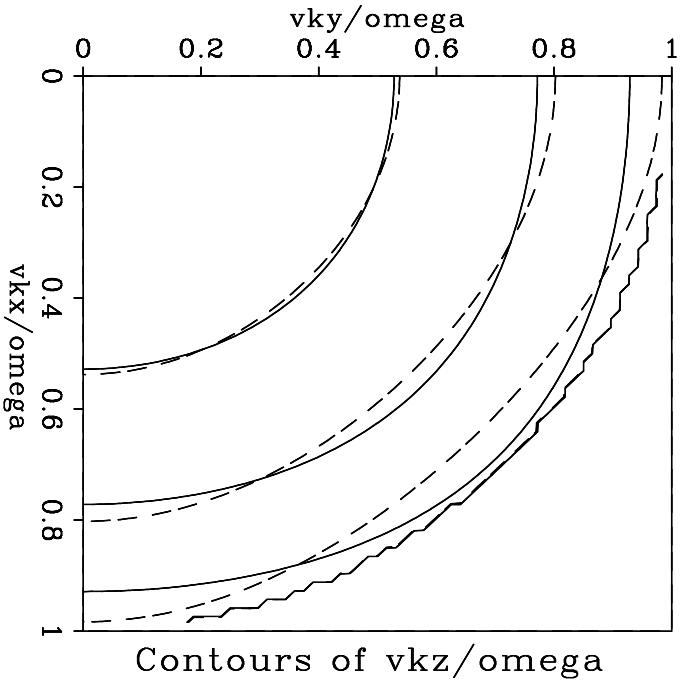

Figure 3: Contours of constant amplitude and phase for the 45-degree splitting approximation described in equation (3) (solid line) and the rotated 45-degree splitting approximation in equation (8)(dashed line). tengli-rot-45 [ER]

The operator obtained by averaging equation (3) and (8) gives

$$\frac{vk_z}{\omega} = \frac{1}{2}\left[2 - \frac{\frac{v^2}{\omega^2}k_x^2}{2 - \frac{v^2k_x^2}{2\omega^2}} - \frac{\frac{v^2}{\omega^2}k_y^2}{2 - \frac{v^2k_y^2}{2\omega^2}} - \frac{\frac{1}{2}\frac{v^2}{\omega^2}(k_x + k_y)^2}{2 - \frac{v^2(k_x+k_y)^2}{4\omega^2}} - \frac{\frac{1}{2}\frac{v^2}{\omega^2}(-k_x + k_y)^2}{2 - \frac{v^2(-k_x+k_y)^2}{4\omega^2}}\right] \tag{9}$$

In Figure **??**, the solid line indicates the contour for the exact 3-D dispersion relation equation (1); the dot-dashed line, the four-pass operator of equation (9). The dispersion relation for the four-pass method looks isotropic but has an error that increases with dip, which is caused by the 45-degree approximation.

THE DIFFERENTIAL EQUATION AND THE DIFFERENCING STAR

Equation (9) applies to downward-going waves. When we do the two-pass and four-pass migration, we apply the exploding reflector concept (Claerbout, 1985), so we use

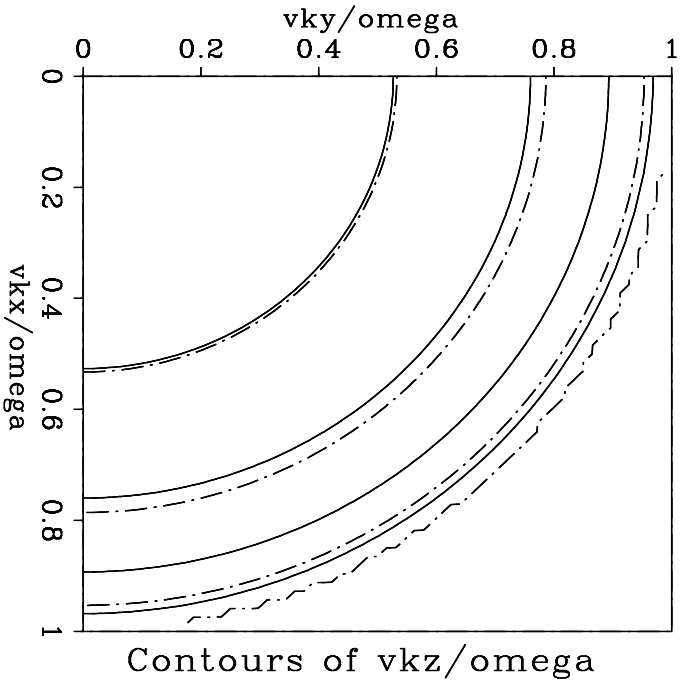

Figure 4: Contours of constant amplitude and phase for the exact 3-D dispersion relation described in equation (1) (solid line) and the averaged 45-degree splitting approximation obtained from the four-pass operator, as in equation (9)(dotted line). tengli-exac-rotavg [ER]

the equation for upward-coming waves instead of the one for downward-going waves.

When the velocity is slowly variable or independent of x and y, the conditions of full separation do apply. The dispersion relation for upward-coming waves can be written as follows:

$$k_z = \frac{1}{2}\left[-2\frac{\omega}{v} + \frac{k_x^2}{2\frac{\omega}{v} - \frac{vk_x^2}{2\omega}} + \frac{k_y^2}{2\frac{\omega}{v} - \frac{vk_y^2}{2\omega}} + \frac{(\frac{k_x+k_y}{\sqrt{2}})^2}{2\frac{\omega}{v} - \frac{v(\frac{k_x+k_y}{\sqrt{2}})^2}{2\omega}} + \frac{(\frac{-k_x+k_y}{\sqrt{2}})^2}{2\frac{\omega}{v} - \frac{v(\frac{-k_x+k_y}{\sqrt{2}})^2}{2\omega}}\right] \tag{10}$$

Using the splitting method, we can separate equation (10) into a thin lens term and a diffraction term as follows:

$$\frac{\partial U}{\partial z} = -i\frac{\omega}{v}U \tag{11}$$

$$\frac{\partial U}{\partial z} = \frac{1}{2}\left[\frac{ik_x^2}{2\frac{\omega}{v} - \frac{vk_x^2}{2\omega}} + \frac{ik_y^2}{2\frac{\omega}{v} - \frac{vk_y^2}{2\omega}} + \frac{ik_x'^2}{2\frac{\omega}{v} - \frac{vk_x'^2}{2\omega}} + \frac{ik_y'^2}{2\frac{\omega}{v} - \frac{vk_y'^2}{2\omega}}\right]U \tag{12}$$

The counterpart of equation (12) in the (ω, x, y, z) domain,

$$\frac{\partial U}{(\partial\frac{z}{2})} = \left[\frac{-i\frac{\partial^2}{\partial x^2}}{2\frac{\omega}{v} + \frac{v\frac{\partial^2}{\partial x^2}}{2\omega}} + \frac{-i\frac{\partial^2}{\partial y^2}}{2\frac{\omega}{v} + \frac{v\frac{\partial^2}{\partial y^2}}{2\omega}} + \frac{-i\frac{\partial^2}{\partial x'^2}}{2\frac{\omega}{v} + \frac{v\frac{\partial^2}{\partial x'^2}}{2\omega}} + \frac{-i\frac{\partial^2}{\partial y'^2}}{2\frac{\omega}{v} + \frac{v\frac{\partial^2}{\partial y'^2}}{2\omega}}\right]U \tag{13}$$

is the equation we use to derive the differencing star and do migration.

For the x and y directions, we use dx, dy, and $dz/2$ to derive the six-point implicit finite-differencing star; for the x' and y' diagonal directions, we use $\sqrt{2}dx$, $\sqrt{2}dy$, and $dz/2$, assuming $dx = dy$. And to minimize frequency dispersion, we use the one-sixth trick (Claerbout, 1985).

IMPLEMENTATION OF THE FOUR-PASS METHOD

To realize the four-pass method, we first apply the diffraction term along the x axis for all y and along the y axis for all x, just as in the two-pass method, except that we use $dz/2$ to get the differencing star. We then sort the data along the x' axis and apply the diffraction term along x' for all y'. Next we sort the data along the y' axis and apply the diffraction term for all x'. Finally, the thin lens term is applied, followed by imaging for each depth.

We use Dave Hale's coding method of the boundary condition (Claerbout, 1985, Page 106) since the zero-slope boundary treatment resulted from taking

$$d(1) = 0. \; ; \; d(nx) = 0.$$
$$endl = -a \; ; \; endr = -c$$

causes the instability after the wave field is downward continued to a certain depth.

COMPARISON OF RESULTS OF THE TWO METHODS

Figure **??** is a depth slice extracted from a 3-D impulse response of the two-pass migration method for a constant velocity medium. Figure **??** is a depth slice at the same depth extracted from a 3-D impulse response of the four-pass method for the same impulse and the same velocity. It is obvious that in Figure **??**, the depth slice of the impulse response is more circular than that in Figure **??**, which demonstrates that the four-pass operator is more isotropic than the two-pass one.

CONCLUSION

Our study demonstrates that the four-pass operator is more isotropic than the two-pass operator. The four-pass technique requires equal spacing along x and y; otherwise, we would have to use interpolation, which could cause artifacts.

In future study, we will compare the four-pass method with Hale-McClellan method.

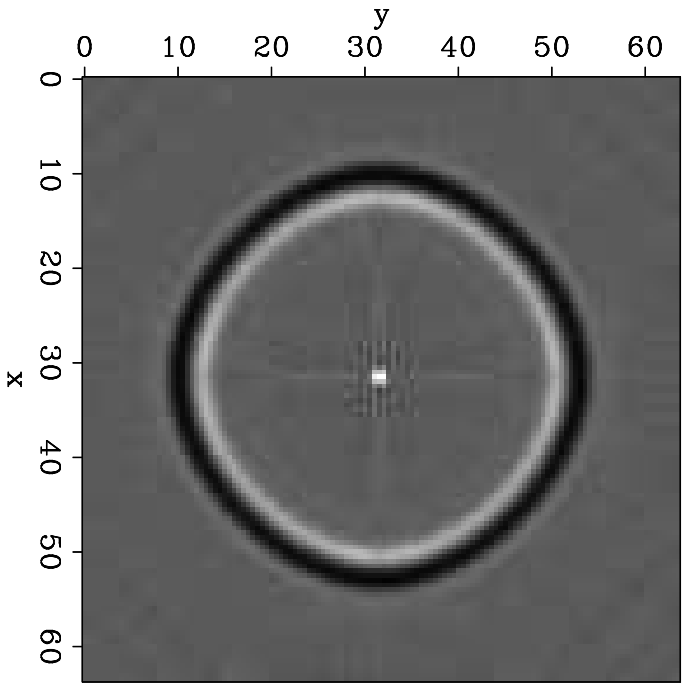

Figure 5: Depth slice from the two-pass technique. tengli-slice220 [CR]

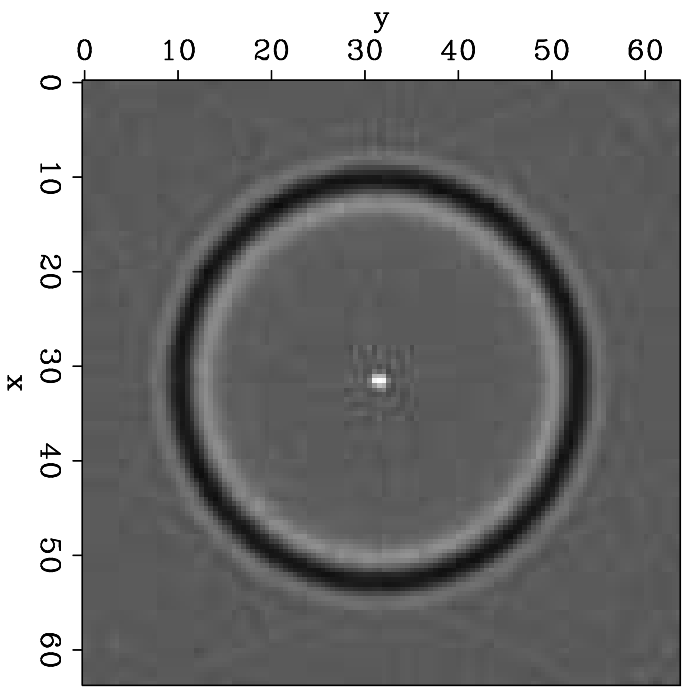

Figure 6: Depth slice from the four-pass technique. It is more circular than that of the two-pass method. Click on the button to see the movie. tengli-slice420 [CR]

ACKNOWLEDGEMENTS

Thanks to Jon Claerbout and Matthias Schwab for many helpful suggestions.

REFERENCES

Brown, D. L., 1983, Applications of operator separation in reflection seismology: Geophysics, **48**, 288–294.

Claerbout, J. F., 1985, Imaging the earth's interior: Blackwell Scientific Publications, Inc.

Ristow, D., 1980, Three-dimensional finite-difference migration: Ph.D. thesis, University of Utrecht.

Yilmaz, O., 1988, Seismic data processing: Soc. Expl. Geophys., Tulsa.